Robust Controller Design for Energy Router in Energy Internet Based on Mixed H_2/H_∞ Control Technique

Chuantong Hao, Haochen Hua, *Member, IEEE*, Yuchao Qin, Junwei Cao, *Senior Member, IEEE*
Research Institute of Information Technology
Tsinghua University
Beijing, P. R. China
jcao@tsinghua.edu.cn

***Abstract*—This paper proposes a new robust controller design of an energy router (ER) system for frequency regulation within an energy Internet (EI) scenario. The studied ER is assumed to be connected with photovoltaic (PV) units, wind turbine generators (WTGs), electrolyzers (ESs), micro-turbines (MTs), fuel cells (FCs), plug in hybrid electric vehicles (PHEVs), loads and one more ER. The intermittent power generation from photovoltaic (PV) units and the random power consumption by PHEVs causes severe frequency oscillation in the considered ER. To alleviate frequency deviation, a proportional integral (PI) controller inside the ER device is designed. For the considered ER system, the inverse output multiplicative perturbation is considered when formulating the H_∞ performance, whereas both minimizing the tracking error and avoiding the situation of over-control are formulated as the H_2 performance. Then our ER control issue is transformed into a mixed H_2/H_∞ control problem which is solved by the particle swarm optimization (PSO) algorithm. Finally, numerical simulations illustrating the feasibility of the proposed methods are provided.**

Keywords—energy Internet, energy routers, microgrids, mixed H_2/H_∞ control, particle swarm optimization

I. Introduction

In the past decades, the global energy crisis and ecological issues have attracted much attention, which has promoted the research of renewable power generation, e.g., wind power, solar power, etc. [1], [2]. Since power generation by photovoltaic (PV) units and wind turbine generators (WTGs) have shortcomings such as low inertia, stochastic, intermittent and uncontrollable [3], [4], the conventional power grids cannot effectively support the access of such distributed renewable energy sources (RESs). Smart grid has enhanced informatization and intellectualization capabilities, providing an appropriate platform for the development and utilization of the RESs; see, e.g., [5].

In recent years, the concept of energy Internet (EI) was proposed [6], and it is considered as the upgraded version of smart grid [7]-[9]. In the EI scenario, customers act as both electric consumers and producers [5], [10]. Through the integration of information and energy, the bi-directional flow and the dynamic balance of energy are realized [8]. It is notable that the core of EI is the energy router (ER) [11], [12], also known as energy hub [13]-[15], or power router [16]. Within an EI, multiple microgrids (MGs) are interconnected via ERs which exchange energy equally [17]. According to the principle of EI operation, the energy routing mechanism is similar to the information exchanging approach in the Internet [18].

Some of the main functions of ERs are to ensure the power quality and to realize an optimized energy management strategy among RESs, energy storage (ES) devices and loads; see, e.g., [19]. Recently, there have been great efforts in studying the energy routing strategies. An energy routing algorithm based on graph theory is designed for energy local area network in [20]. In [21], a series of energy routing strategy is investigated for delay-tolerant loads and mobile energy buffers. The problem of power quality control in distribution grid based on ER was investigated in [22]. An economic based energy routing strategy has been proposed in [23]. Steady-state power flow model of ER embedded AC network and its application in optimizing power system operation has been reported in [24].

It is notable that most of the existing literatures with respect to (w.r.t.) the investigation of ERs focus on either routing algorithms or the field of power electronics. There have been few work investigating energy management issues for ERs from the control perspective. Within an EI scenario, a typical ER is allowed to have access to multiple PV units, WTGs, micro-turbines (MTs), fuel cells (FCs), plug in hybrid electric vehicles (PHEVs), electrolyzers (ESs), loads, and other ERs [11]-[15]. Since PV power generation is influenced by solar irradiation, WTG power generation is affected by power of wind, and load power is disturbed by the access of a large number of PHEVs, power deviation in the ER would cause its AC bus frequency oscillation. In this sense, an effective controller in ER is required to regulate the AC bus frequency. Besides, the sum of tracking error and the additional cost involved by the controller itself shall be minimized. The problem of designing a controller such that the aforementioned challenges are solved has not been fully investigated.

In this paper, a scenario of ER which is connected with PV units, WTGs, ESs, MTs, FCs, PHEVs, loads and one more ER is studied. We design proportional integral (PI) ER controller

(ERC) based on a mixed H_2/H_∞ control technique. Inverse output multiplicative perturbation is considered in formulating the H_∞ performance of the studied ER system. Both tracking error and the cost of controllers are considered to be minimized, which is formulated as the H_2 performance. To obtain the optimal solution, particle swarm optimization (PSO) algorithm [27] is utilized. In this sense, the optimal robust controller is obtained.

The rest of the paper is organized as follows: Section II introduces the ER system modeling. Problem formulation and solutions are given in Section III. In Section IV, numerical examples are illustrated. Finally, Section V concludes the paper.

II. System Modeling

In this section, we focus on a typical scenario of ER which has access to PV units, WTGs, ESs, MTs, FCs, PHEVs, loads and the other ER (denoted as ER_2) via converters, shown in Fig. 1. Ordinary differential equations (ODEs) are applied to describe the dynamic performance of the studied ER system.

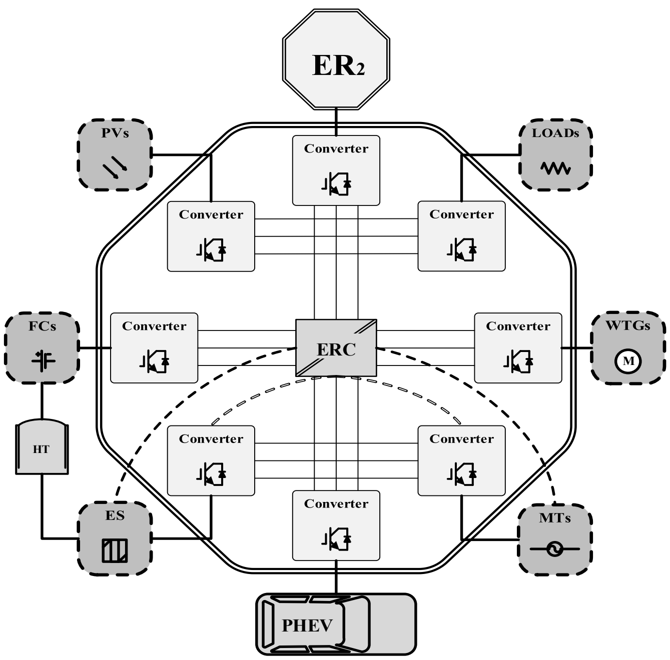

Fig. 1. The scenario of the studied ER.

In Fig. 1, large-scale RESs such as PV units and WTGs are utilized as the main power generator devices. Whenever power generation by RESs cannot support the usage of loads, the controllable MTs and FCs are utilized to generate power, such that the power balance of the considered ER is achieved. ESs are used to consume superfluous electric power to produce hydrogen which is environmentally friendly. The hydrogen tanks (HTs) are applied to store hydrogen for FC power generation. A variety of PHEVs with different charging strategies and states can be treated as a class of special loads with relatively large power deviation. Besides, the studied ER has access to normal loads such as factories or buildings. Although the power flow between two interconnected ERs is highly controllable, the energy routing strategy shall not be frequently changed, since energy switching itself is relatively costly. Since our research is focused on the dynamical ER system, (normally the considered time period is no more than 3000s), we assume that the studied ER supplies constant power to ER_2. The ERC is designed to control the output power of ESs and MTs. In addition, the FC output power is assumed to be a constant value. Such consumption has been made in many works [29] [30].

Large frequency deviation (Δf) of ER may cause serious problems such as ER system blackout. Since Δf is mainly affected by the AC bus power fluctuation (ΔP), frequency stabilization can be achieved by keeping ER system power balance. The total power generation and consumption of the studied ER is denoted as P_G and P_L, respectively. Notations P_{PV}, P_{WTG}, P_{FC} and P_{MT} represents for power generation of PVs, WTGs, FCs and MTs, respectively. Notations P_{ES}, P_{ER_2}, P_{PHEV} and P_{LOAD} stand for power consumption of ESs, ER_2, PHEVs and loads, respectively. Thus, the following equations hold:

$$P_G = P_{PV} + P_{WTG} + P_{FC} + P_{MT}, \tag{1}$$

$$P_L = P_{ES} + P_{ER2} + P_{PHEV} + P_{LOAD}, \tag{2}$$

$$\Delta P = P_G - P_L. \tag{3}$$

We denote the power change of ES consumption, FC generation and MTs generation as ΔP_{ES}, ΔP_{FC} and ΔP_{MT}, respectively. K_{ES}, K_{FC} and K_{MT} stand for the gain of ESs, FCs and MTs, respectively. ES and MT control output signal are denoted as ΔP_{ESC} and ΔP_{MTC}, respectively. T_{ES} represents for the time constant of ESs. Damping coefficient and inertia constant are denoted as D and M, respectively. The PI controllers in ERC are denoted as K_{MTC} and K_{ESC}, utilized to control MTs and FCs respectively. Referring to a battery-energy-storage facility, ΔP_{ES} and ΔP_{FC} are approximated by a first order transfer function [25], as is shown in (4) and (5),

$$\Delta P_{ES} = \frac{K_{ES}}{1 + T_{ES}s}\Delta f, \tag{4}$$

$$\Delta P_{FC} = \frac{K_{FC}}{1 + T_{FC}s}\Delta f. \tag{5}$$

Take the linear power versus frequency droop characteristics into consideration, ΔP_{MT} is obtained by:

$$\Delta P_{MT} = \frac{1}{-K_{MT}}\Delta f. \tag{6}$$

A linearized block diagram is formulated in Fig. 2. The power dynamic of ESs and ER frequency deviation Δf can be formulated as follows.

$$\begin{cases} \Delta\dot{P}_{ES} = -\dfrac{1}{T_{ES}}\Delta P_{ES} + \dfrac{K_{ES}}{T_{ES}}\Delta f, \\ \Delta\dot{f} = -\dfrac{1}{M}\Delta P_{ES} - \dfrac{D\cdot K_{MT}+1}{M\cdot K_{MT}}\Delta f + \dfrac{1}{M}\Delta P_{ESC} \\ \qquad + \dfrac{1}{M}\Delta P_{MTC}. \end{cases} \tag{7}$$

Besides, we have

$$\Delta P = -\Delta P_{ES} - \frac{1}{K_{MT}}\Delta f + \Delta P_{ESC} + \Delta P_{MTC}. \tag{8}$$

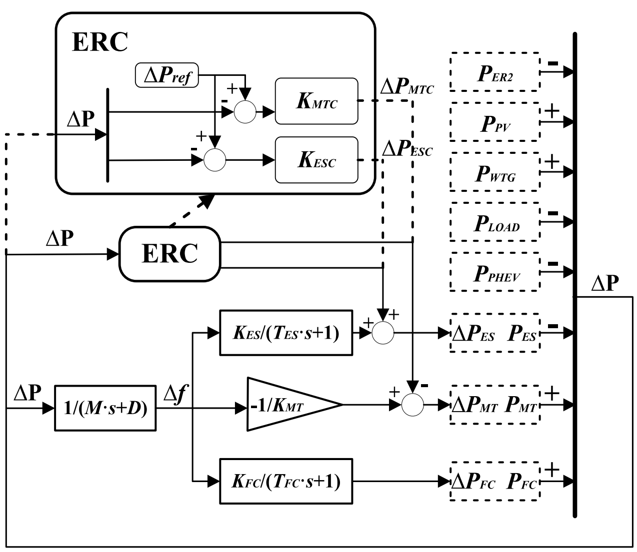

Fig. 2. Linearized block diagram of ER system.

To simplify the dynamical equations (7) and (8), state vector $x(t)$, output vector $\mathrm{y}(t)$ and control output $u(t)$ are defined as follows: (time t omitted)

$$x = \begin{bmatrix}\Delta P_{ES} \\ \Delta f\end{bmatrix}, \qquad \mathrm{y} = \Delta P, \qquad u = \begin{bmatrix}\Delta P_{ESC} \\ \Delta P_{MTC}\end{bmatrix}.$$

Observing (7) and (8), the studied ER system can be transformed into the following mathematical control system:

$$\begin{cases} \dot{x} = Ax + Bu, \\ y = Cx + Du, \end{cases} \tag{9}$$

where

$$A = \begin{bmatrix} -\dfrac{1}{T_{ES}} & \dfrac{K_{ES}}{T_{ES}} \\ -\dfrac{1}{M} & -\dfrac{D\cdot K_{MT}+1}{M\cdot K_{MT}} \end{bmatrix}, \qquad \mathrm{B} = \begin{bmatrix} 0 & 0 \\ \dfrac{1}{M} & \dfrac{1}{M} \end{bmatrix},$$

$$C = \begin{bmatrix} -1 & -\dfrac{1}{K_{MT}} \end{bmatrix}, \qquad D = [1 \quad 1].$$

PI controllers are applied to the ERC, the control output signal and controller of ESs and MTs are as follows:

$$\Delta P_{ESC} = K_{ESC}(s)\cdot\Delta P, \tag{10}$$

$$\Delta P_{MTC} = K_{MTC}(s)\cdot\Delta P, \tag{11}$$

$$K_{ESC}(s) = K_{P_{ES}} + \frac{K_{I_{ES}}}{\mathrm{s}}, \tag{12}$$

$$K_{MTC}(s) = K_{P_{MT}} + \frac{K_{I_{MT}}}{\mathrm{s}}. \tag{13}$$

The ER system in (9) is a multi-input-single-output (MISO) controlled system with the nominal plant of G and the controller transfer function K.

III. Problem Formulation and Solution

In this section, inverse output multiplicative perturbation and tracking error are utilized to evaluate the H_∞ and H_2 performances, respectively. By minimizing the cost function by PSO algorithm, the optimal controller's parameters are figured out.

A. Mixed H_2/H_∞ Control Technique

Consider the control system of ER with external disturbance, as is shown in Fig. 3. G is the nominal plant and K is the ERC controller introduced in Section II. Reference input, tracking error, control output, external disturbance and system output are represented by $r(t)$, $e(t)$, $u(t)$, $d(t)$ and $y(t)$, respectively.

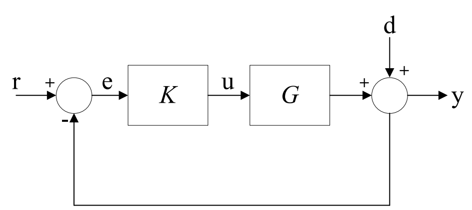

Fig. 3. Control system of ER .

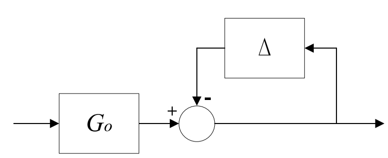

Fig. 4. Inverse output multiplicative perturbation configuration.

Besides, system uncertainties caused by parameters measurement error and various power oscillation are considered.

Assume that the unstructured uncertainties of the plant is modeled by multiplicative uncertainty denoted as block Δ. Inverse output multiplicative perturbation [31] is introduced here to evaluate the robust control effect, as is shown in Fig. 4. G_0 is the open-loop transfer function of the controlled ER system, and $G_0 = GK$.

The small gain theorem implies that a system with stable multiplicative uncertainties is stable if (14) holds:

$$\|\Delta \cdot (I + GK)^{-1}\|_\infty < 1. \quad (14)$$

Then we have:

$$\|\Delta\|_\infty < \frac{1}{\|(I + GK)^{-1}\|_\infty}.$$

The robust stability margin against the system uncertainties is express by the value of $1/\|(I + GK)^{-1}\|_\infty$. The robust stability margin of the closed-loop system can be maximized by minimizing $\|(I + GK)^{-1}\|_\infty$, based on which, the robust H_∞ controller is obtained. The H_∞ control cost function is formulated as J_∞,

$$J_\infty = \|(I + GK)^{-1}\|_\infty. \quad (16)$$

To further improve the system control performance, apart from considering robust stability and disturbance attenuation, the minimization of tracking error should be taken into account [26]. The tracking error is formulated as

$$J_e = \int_0^\infty e'(t)e(t)dt = \|E(s)\|_2^2, \quad (17)$$

where $e(t) = r(t) - y(t)$ is the tracking error. Let $\Delta = 0$ and $d(t) = 0$, from the inverse Laplace transformation of $E(s)$,

$$E(s) = (I + GK)^{-1}R(s) \quad (18)$$

$e(t)$ can be figured out.

Since oversized controllers in ERC may cause excessive loss of hardware equipment in ER system [28], the additional cost involved by the controller shall be considered. The cost function J_k is utilized to estimate the cost of the desired controller.

$$J_k = \left[\left(K_{P_{ES}} + K_{P_{MT}}\right) \cdot \left(K_{I_{ES}} + K_{I_{MT}}\right)\right]^2 \quad (19)$$

The H_2 control cost function is formulated by the sum of tracking error value and the cost involved by controller, denoted as $J_2 = J_e + \varepsilon \cdot J_k$. Here ε is the weight coefficient. In order to achieve robust stablization and optimal tracking performance of the ER system, as well as to avoid the situation of over-control, we formulate our targets into the mixed H_2/H_∞ control problem whose objective function is defined as:

$$J = J_2 + J_\infty. \quad (20)$$

Then, our target is to minimise J in (20) subject to

$$K_{P_{ES},min} < K_{P\_ES} < K_{P_{ES},max},$$

$$K_{I_{ES},min} < K_{I_{ES}} < K_{I_{ES},max},$$

$$K_{P_{MT},min} < K_{P_{MT}} < K_{P_{MT},max},$$

$$K_{I_{MT},min} < K_{I_{MT}} < K_{I_{MT},max},$$

In the above inequalities, $K_{P_{ES},min}$ and $K_{I_{ES},min}$ are the minimum gains of proportional part and integral part in ERC to control ES. $K_{P_{MT},min}$ and $K_{I_{MT},min}$ are the minimum gains of proportional part and integral part in ERC to control MT. $K_{P_{ES},max}$ and $K_{I_{ES},max}$ are the maximum gains of proportional part and integral part in ERC to control ES, $K_{P_{MT},max}$ and $K_{I_{MT},max}$ are the maximum gains of proportional part and integral part in ERC to control MT. Weighting coeffieient ε is set to be 0.1. The values of $K_{P_{ES}}$, $K_{I_{ES}}$, $K_{P_{MT}}$ and $K_{I_{MT}}$ are tuned by the PSO algorithm.

B. PSO Algorithm

PSO is an evolutionary algorithm starting from a random solution and finding the optimal solution by iteration [27]. The quality of solution is evaluated through the fitness. PSO finds the global optimum by following the currently searched best value. Due to its high precision and fast convergence, PSO has attracted the attention of the academic community, and has shown its superiority in solving practical problems; see, e.g., [32]. The flowchart of PSO algorithm is shown in Fig. 5.

The fitness value of particles is calculated by the mixed H_2/H_∞ control objective function (20). The best previously visited position of particle i is marked as $pbest_i$. The position of the best individual of the whole swarm is defined as the global best position, marked as $gbest_i$. The velocity and new position of particle i, represented by v_i and x_i, are updated by the following equations:

$$v_{i+1} = w \cdot v_i + c_1 \cdot rand_1 \cdot (pbest_i - x_i) + c_2 \cdot rand_2 \cdot (gbest_i - x_i), \quad (20)$$

$$x_{i+1} = x_i + v_{i+1}, \quad (21)$$

with

$$w = w_{max} - \frac{w_{max} - w_{min}}{iter_{max}} iter,$$

where c_1 and c_2 are the cognitive and social acceleration factors, respectively. $rand_1$ and $rand_2$ are the random numbers of range (0,1). w is the inertia weight factor. w_{min} and w_{max} are the minimum and maximum of inertia weight factors, respectively. $iter$ and $iter_{max}$ are the iteration count and maximum iteration, respectively.

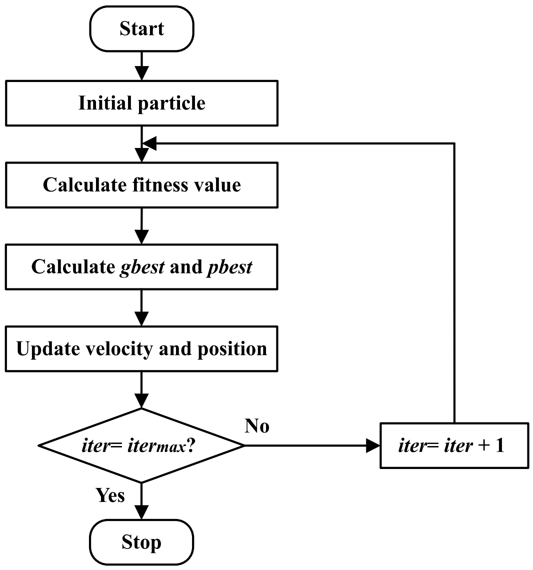

Fig. 5. Flowchart of PSO algorithm.

The PSO based mixed H_2/H_∞ controller design procedure is presented as follows:

1) Initialize particles with random positions and velocities.

2) Evaluate the objective function in (20) for each particle. MATLAB μ-Analysis and Synthesis Toolbox is utilized to evaluate the H_∞-norm and H_2-norm in objective function J.

3) Compare the fitness value of each particle with $pbest_i$. The best fitness value among all the $pbests$ is $gbest$.

4) Update the velocity v_i and position of particle x_i.

5) Stop the circulation when $iter_{max}$ is arrived. Otherwise go to process 2.

In this paper, the minimum boundary of PI controller ($K_{P_{ES},min}$, $K_{I_{ES},min}$, $K_{P_{MT},min}$, $K_{I_{MT},min}$) is set at 0.0001. The maximum value ($K_{P_{ES},max}$, $K_{I_{ES},max}$, $K_{P_{MT},max}$, $K_{I_{MT},max}$) is set to be 1. The swarm size and maximum iteration are set to be 50 and 30, respectively. The values of c_1, c_2, w_{min} and w_{max} are set to be 2, 2, 0.4 and 0.9, respectively.

IV. Simulation Results

In this section, the optimal parameters of the controller are figured out by via PSO algorithm. Several typical simulation results are presented to demonstrate the feasibility of the proposed scheme. The system parameters are mainly based on the data in [29], as is shown in Table I.

We choose $R(s) = 1/(s + 1.1)$ as the reference input of the ERC system. The objective function value versus iteration is shown in Fig. 6. Based on the optimum solution of PSO, the optimal value of J is 0.8827, and the mixed H_2/H_∞ controller proposed in this paper is as follows:

$$K_{ESC}(s) = 0.3372 + \frac{0.9916}{s} \tag{23}$$

$$K_{MTC}(s) = 0.2775 + \frac{0.5653}{s} \tag{24}$$

TABLE I. System Patameters

ESs		**FCs**		**MTs**	
P_{ES}^{ini}	50kW	P_{FC}^{ini}	5kW	P_{MT}^{ini}	70kW
P_{ES}^{max}	70kW	P_{FC}^{max}	5kW	P_{MT}^{max}	200kW
P_{ES}^{min}	30kW	P_{FC}^{min}	2kW	P_{MT}^{min}	10kW
K_{ES}	100			K_{MT}	0.04
T_{ES}	60			M	10
				D	1
PV		**WTGs**		**ER2**	
P_{PV}^{ini}	25kW	P_{WTG}^{ini}	25kW	P_{ER2}^{ini}	50kW
P_{PV}^{max}	50kW	P_{WTG}^{max}	50kW	P_{ER2}^{max}	50kW
P_{PV}^{min}	10kW	P_{WTG}^{min}	10kW	P_{ER2}^{min}	20kW
PHEV		**Loads**		**System**	
P_{PHEV}^{ini}	15kW	P_{LOAD}^{ini}	10kW	f_0	50Hz
P_{PHEV}^{max}	100kW			$Base$	150kW

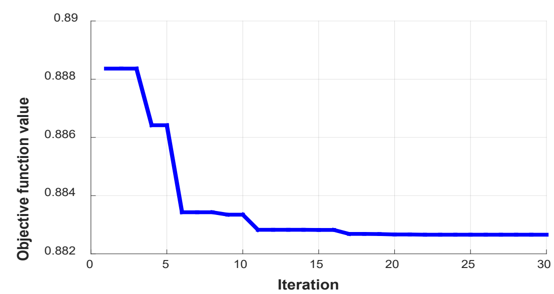

Fig. 6. Objective function value versus iteration.

Power of PV units, WTGs and loads are simulated by a forecasted model with random fluctuations [29], illustrated in Fig. 7, Fig. 8 and Fig. 9, respectively. The model of PHEV power deviation is derived from white noise block with a band pass filter. The power fluctuation of PHEV is presented in Fig. 10.

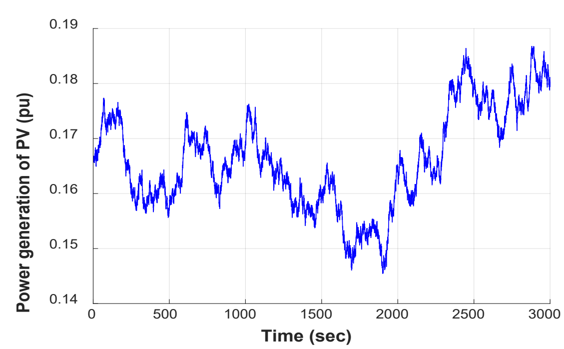

Fig. 7. Power fluctuation of PV.

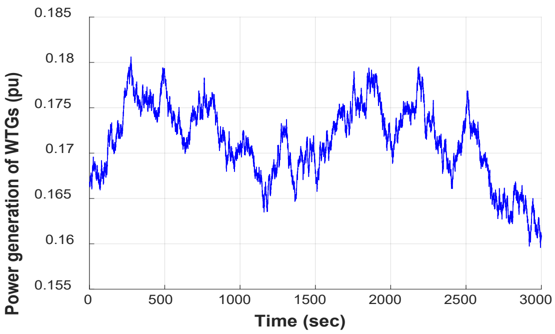

Fig. 8. Power fluctuation of WTGs.

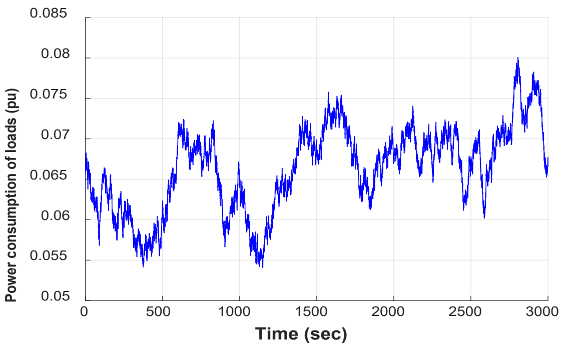

Fig. 9. Power fluctuation of loads.

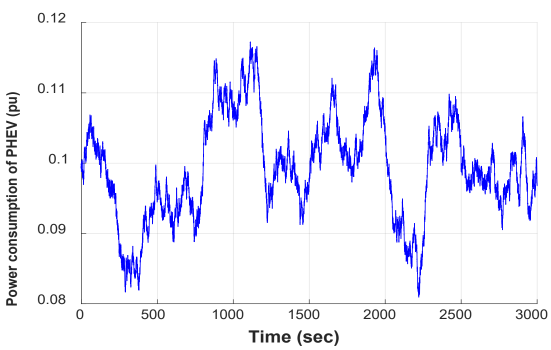

Fig. 10. Power fluctuation of PHEV.

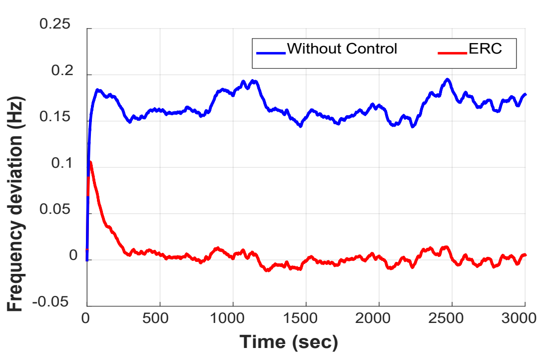

Fig. 11. Frequency deviation without control and with ERC.

Assume that the ER system power is unbalanced at initial time. The AC bus frequency deviations with and without control are shown in Fig. 11. Obviously, the proposed ERC scheme achieve the frequency stabilization effectively. In the simulation, the control effect of ERC is compared with that of control system of MT and ES (CMT&CES) [29] and robust MT and ES controller (RMT&RES) [30].

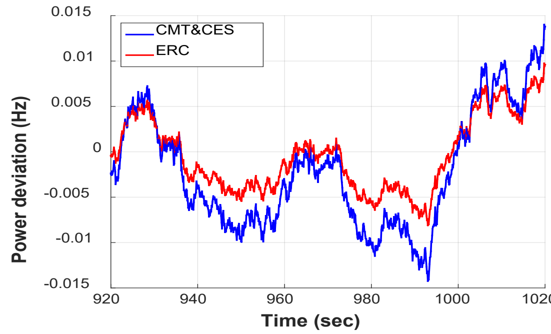

Fig. 12. System power deviation under the CMT&CES and ERC controls.

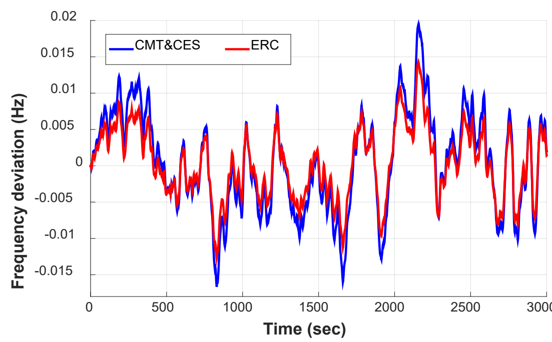

Fig. 13. Frequency deviation under the CMT&CES and ERC controls.

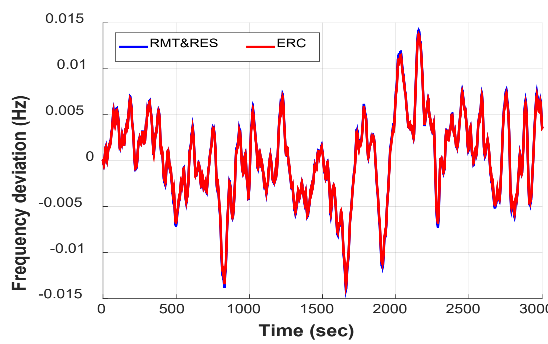

Fig. 14. Frequency deviation under the RMT&RES and ERC controls.

System power and frequency deviation under CMT&CES and ERC are illustrated in Fig. 12 and Fig. 13, respectively. From Fig. 11 and Fig. 13, we see that the power usage in ER could be balanced more efficiently under ERC than that under CMT&CES. Besides, the frequency oscillations are damped more efficiently with ERC. Frequency deviation under the RMT&RES and ERC are illustrated in Fig. 14. The results imply that the H_∞ control effect of the two schemes is quiet close. However, the additional cost involved by the controller in ERC and in RMT&RES are 0.9228 and 1.8317, respectively. Reducing the cost to approximately half of that in RMT&RES,

the superiority of our proposed method is demonstrated distinctly.

V. Conclusion

In this paper, a new robust controller design of dynamical ER system has been presented. The PSO-based mixed H_2/H_∞ control technique is applied to optimize the PI control parameters of ERC. Simulations show that our target is achieved.

Acknowledgment

This work was supported in part by National Natural Science Foundation of China (grant No. 61472200) and Beijing Municipal Science & Technology Commission (grant No. Z161100000416004).

References

[1] S. Bilgen, K. Kaygusuz, and A. Sari, “Renewable energy for a clean and sustainable future,” *Energy Sources*, vol. 26, no. 12, pp. 1119-1129, 2004.

[2] G. Zhabelova, V. Vyatkin, and V. N. Dubinin, “Toward industrially usable agent technology for smart grid automation,” *IEEE Trans. Industrial Electronics*, vol. 62, no. 4, pp. 2629-2641, Apr. 2015.

[3] G. Venkataramanan and C. Marnay, “A larger role for microgrids,” *IEEE Power Energy Mag.*, vol. 6, no. 3, pp. 78–82, May 2008.

[4] S. Park, J. Lee, G. Hwang, and J. K. Choi, “Contribution-based energy-trading mechanism in microgrids for future smart grid: a game theoretic approach,” *IEEE Trans. Ind. Electron.*, vol. 63, no. 7, pp. 4255-4265, Jul. 2016.

[5] W. Tushar, B. Chai, C. Yuen, D. B. Smith, K. L. Wood, Z. Yang, and H. V. Poor, “Three-party energy management with distributed energy resources in smart grid,” *IEEE Trans. Ind. Electron.*, vol. 62, no. 4, pp. 2487-2498, Apr. 2015.

[6] J. Rifkin, “The third industrial revolution: how lateral power is transforming energy, the economy, and the world,” *Palgrave Macmillan*, New York, pp. 31-46, 2013.

[7] A. Q. Huang, M. L.Crow, G. T. Heydt, J. P. Zheng, and S. J. Dale, “The future renewable electric energy delivery and management (FREEDM) syetem: the energy internet,” in *Proc. IEEE*, vol. 99, no. 1, pp. 133-148, Nov. 2010.

[8] J. Cao and M. Yang, “Energy Internet - towards smart grid 2.0,” in Proc. *Fourth Int. Conf. Networking & Distributed Computing*, Los Angeles, USA, Dec. 2013, pp. 105–110.

[9] L. H. Tsoukalas and R. Gao, “From smart grids to an energy Internet - assumptions, architectures and requirements,” *Smart Grid and Renewable Energy*, vol. 1, pp. 18–22, Sept. 2009.

[10] C. Tham, and T. Luo, “Sensing-driven energy purchasing in smart grid cyber-physical system,” *IEEE Trans. Systems, Man, and Cybernetics,* vol. 43, no. 4, pp. 773-784, Jul. 2013.

[11] Y. Xu, J. Zhang, W. Wang, A. Juneja, and S. Bhattacharya, “Energy router: architectures and functionalities toward energy internet”, in *Proc. 2011 IEEE Int. Conf. on Smart Grid Commun.*, Brussels, Belgium, Oct. 2011, pp.31-36.

[12] Y. Ma, X. Wang, X. Zhou, and Z. Gao, “An overview of energy routers,” in *Proc. 29th Chinese Control and Decision Conf.*, Chongqing, China, May 2017, pp. 4104-4108.

[13] M. Geidl, G. Koeppel, P. Favre-Perrod, and B. Klokl, “Energy hubs for the futures,” *IEEE Power & Energy Mag.*, vol. 5, no. 1, pp. 24 -30, Jan.-Feb. 2007.

[14] P. Favre-Perrod, “A vision of future energy networks,” in *Proc. Power Eng. Soc. Inaugural Conf. Expo Africa*, Durban, South Africa, Jul. 2005, pp. 13-17.

[15] M, Schulze, L. Friedrich, and M, Gautschi, “Modeling and optimization of renewable: applying the energy hub approach,” in *Proc. IEEE Int. Conf. Sustainable Energy Technologies*, Singapore, Nov. 2008, pp. 83-88.

[16] J. Boyd, “An internet-inspired electricity grid”, *IEEE Spectrum*, vol. 50 no. 1, pp. 12-14, 2013.

[17] J. Miao, N. Zhang, and C. Kang, “Generalized steady-state model for energy router with applications in power flow calculation,” in *Porc. Power and Energy Society General Meeting*, Boston, USA, Jul. 2016, pp. 1-5.

[18] X. Han, F. Yang, C. Bai, G. Xie, G. Ren, H. Hua, *et al.*, “An open energy routing network for low-voltage distribution power grid,” in *Proc. 1st IEEE Int. Conf. on Energy Internet*, pp. 320-325, Beijing, China, Apr. 2017.

[19] H. Hua, J. Cao, G. Yang, and G. Ren, “Voltage control for uncertain stochastic nonlinear system with application to energy Internet: Non-fragile robust H_∞ approach,” *J. Math. Anal. Appl.*, https://doi.org/10.1016/j.jmaa.2018.03.002, in press.

[20] R. Wang, J. Wu, Z. Qian, and Z. Lin, “A graph theory based energy routing algorithm in energy local area network,” *IEEE Trans. Ind. Inform.*, vol. 13, no. 6, pp. 3275-3285, Dec. 2017.

[21] M. Erol-Kantarci, J. H. Sarker, and H. T. Mouftah, “Energy routing in the smart grid for delay-tolerant loads and mobile energy buffers,” in *Proc. 2013 IEEE Symp. on Computers and Communications*, Split, Croatia, Jul. 2013, pp. 149-154.

[22] Q. Duan, C. Ma, W. Sheng, and C. Shi, “Research on power quality control in distribution grid based on energy router,” in *Proc. 2014 Int. Conf. on Power System Technology*, Chengdu, China, Oct. 2014, pp. 2115-2121.

[23] S. Hambridge, A. Q. Huang, and R. Yu, “Solid state transformer (SST) as an energy router: economic dispatch based energy routing strategy,” in *Proc. 2015 IEEE Energy Conversion Congress and Exposition*, Montreal, Canada, Sept. 2015, pp. 2355-2360.

[24] J. Miao, N. Zhang, C. Kang, J. Wang, Y. Wang, and Q. Xia, “Steady-state power flow model of energy router embedded AC network and its application in optimizing power system operation,” *IEEE Trans. Smart Grid*, DOI 10.1109/TSG.2017.2672821, in press.

[25] D. Kottick, M. Blau, D. Edelstein, “Battery energy storage for frequency regulation in an island power system,” *IEEE Trans. Energy Convers.*, vol. 8, no. 3, pp. 455-458, Sep. 1993.

[26] S. J. Ho, S. Y. Ho, M. H. Hung, L. S. Shu, H.L. Huang, “Designing structure-specified mixed H_2/H_∞ optimal controllers using an intelligent genetic algorithm IGA,” *IEEE Trans. Control Syst. Technol*., vol. 13, no. 6, pp. 1119-1124, Nov. 2005.

[27] J. Kennedy and R. Eberhart, “Particle swarm optimization,” in *Proc. IEEE Int. Conf. Neural Networks,* Perth, Australia, Nov.-Dec. 1995, pp. 1942-1948.

[28] H. Hua, Y. Qin, and J. Cao, “A class of optimal and robust controller design for islanded microgrid,” in *Proc. IEEE 7th Int. Conf. on Power and Energy Syst.*, Toronto, Canada, Nov. 2017, pp. 111-116.

[29] X. Li, Y. J. Song, and S. B. Han “Study on power quality control in multiple renewable energy hybrid microgrid system,” in *Proc. IEEE Lausanne Power Tech.*, Lausanne, Switzerland, Jul. 2007, pp. 2000-2005.

[30] S. Vachirasricirikul and I. Ngamroo, “Robust controller design of micro turbine and electrolyzer for frequency stabilization in a micro grid system with plug-in hybrid electric vehicles,” *Int. J. Elect. Power Energy Syst.*, vol. 43, no. 1, pp. 804-811, Dec. 2012.

[31] D. W. Gu, P. Hr. Petkov, and M. M. Konstantinov, *Robust Control Design With MATLAB*, Springer, New York, Feb. 2005.

[32] B. T. Thanh and M. Parnichkun, “Balancing control of bicyrobo by particle swarm optimization-based structure-specified mixed H_2/H_∞ control,” *Int. J. Adv. Robot. Syst.*, vol. 5, no. 4, pp. 395-402, 2008.